Tribology International 43 (2010) 178–187

Contents lists available at ScienceDirect

Tribology International

journal homepage: www.elsevier.com/locate/triboint

Application of micro-ball bearing on Si for high rolling life-cycle

Sujeet K. Sinha [a,*], Robin Pang [a], Xiaosong Tang [b]

[a] Department of Mechanical Engineering, National University of Singapore, 9 Engineering Drive 1, Singapore 117576, Singapore
[b] Institute of Materials Research and Engineering, Singapore

ARTICLE INFO

Article history:
Received 17 November 2008
Received in revised form
9 April 2009
Accepted 8 May 2009
Available online 18 May 2009

Keywords:
Micro-ball bearing
Wear life-cycle

ABSTRACT

In this paper, we introduce a new class of micro-ball bearing that can be applied between two Si surfaces in relative motion where wear is a problem. Wide channel was created on one Si plate for all the ball bearings to roll within this channel rather than in individual grooves. This type of micro-bearings can be applied as friction reducers to micro- and nano-machines. The tribometer set-up consisted of a top plate (Si wafer), which was connected to a conventional bearing, resting on a bottom plate (also Si wafer) that was rotated at 300 and 500 RPM by a DC motor. Borosilicate glass micro-spheres, $53 \pm 3.7\,\mu m$ in diameter, were rotated between the two circular silicon plates (15 mm diameter) under a dead weight of 235 μN and in high-humidity conditions (75% relative humidity (RH)). Tests on the plate with wide channel consistently exceeded 1 million cycles of rotation without failure of the bearing. The main factors affecting the life-cycle are identified as the presence of a wide channel, ball dispersion, and alignment of the Si plates.

1. Introduction

The reliability of mircosystems, such as micro-electromechanical systems (MEMS), is a major stumbling block in the fast development of this technology for wider applications. Challenges that need to be overcome include tribological problems such as adhesion, friction, capillary, and stiction phenomena in humid conditions, and, especially, wear from rubbing contacts [1–8]. To avoid these surface-related problems, successfully commercialized MEMS are essentially designed to avoid dynamic contact, for example, Texas Instrument's Digital Micromirror Device [9]. Such designs have greatly limited the potential of MEMS. There is still no solution to effectively solve the above-mentioned problems and especially that of stiction, friction, and wear which might be slowing down the progress of MEMS commercialization [10–12]. Self-assembled monolayer films have been instrumental in reducing adhesion and wear problems at the silicon interfaces. Yet, their wear performance and robustness for prolonged sliding cycles in harsher conditions are still major issues [4,5,13,14]. Therefore, the "micro-ball bearing" has some potential due to its low rolling resistance when compared with sliding. The eventual success of any such technique, nevertheless, lies in the feasibility of the deposition step during fabrication, and in reliable performance with longer wear life [5,15].

Various authors have experimented with the idea of using micro- or nano-spheres such as fullerenes ($C_{60,}$ K_{60}) [16], or nano-balls (MoS_2 and WS_2), as ball bearings and lubricating agents in the industry [17]. Work conducted on the frictional characteristics of WS_2 and MoS_2 nano-balls by Rapoport et al. [18,19] shows plastic deformation to the nano-balls, indicative of sliding rather than rolling. Low friction in their case is primarily achieved by the peeling of WS_2 or MoS_2 layer which constitute these nano-balls. Moreover, WS_2 and MoS_2 are well-known solid lubricants. Molecular dynamics simulation studies [16,20] on molecular nano-balls have been conducted to study their potential in small machines. Their reliabilities under longer rolling cycles however, have not been investigated experimentally. From these simulation studies, we can see that ball bearings are robust and that they can help reduce wear due to rolling contact. Glass micro-spheres have been investigated by NASA as lubrication for space applications in journal bearings [21]. The frictional property of micro-spheres was investigated by Ghodssi et al. [22–24] and Beerschwinger et al. [15] for MEMS. Beerschwinger reported coefficient of rolling friction for glass micro-spheres of about 0.05, and Ghodssi a value of 0.01 for steel spheres. Other groups currently working on rolling elements include Kim et al. on cylindrical bearings [14] and Miura and Kamiya on fullerenes nano-bearings [25]. Recently, the success of introducing polystyrene micro-spheres as spacers in preventing stiction in MEMS marks the first time that micro-spheres are being deposited and successfully tested in actual MEMS devices [26].The focus of this paper is to show the ability of the micro-spheres to roll for prolong rotational cycles simulating actual device life. This is being characterized by the duration (number of cycles of revolutions of the planar disk) for which the balls can roll between two flat circular silicon plates with a dead-weight load acting. Circular channel, much wider than the

* Corresponding author.
E-mail address: mpesks@nus.edu.sg (S.K. Sinha).

0301-679X/$ - see front matter © 2009 Elsevier Ltd. All rights reserved.
doi:10.1016/j.triboint.2009.05.015

diameter of the balls, has also been added to compare the difference in performance between balls rolling in a channel and without. The performance of balls rolling in the wide channel shows far superior life-cycle. Strong adhesion forces exist between the balls and the silicon plates which help keep the balls between the plates. The surface forces are mainly due to capillary force from meniscus that forms in a humid environment. Other forces that are also present include electrostatic [27], magnetic, and viscous forces. The surface forces do not hinder the rolling action of the balls in any way as the resistive threshold force for rolling is far less than that for sliding. Even at nanometers size of bearing materials, such as cylindrical carbon nanotube, research [28] has shown that rolling can be achieve by a suitable application of tangential force despite strong surface adhesion. A rotary tribometer has been built for evaluating the performance of the bearings. Factors affecting the life-cycle of this bearing system under different test conditions are analyzed and characterized here. We have tested on $53 \pm 3.7\,\mu m$ borosilicate glass micro-spheres between silicon plates for with and without the wide channel and studied the total life-cycle. Present results are clear evidences of the potential of these micro-ball bearings to solve frictional problems in MEMS or similar microsystem devices.

2. Some theoretical considerations

As objects become smaller in size, the surface to volume ratios increase and therefore, the dominance of the gravitational force gives way to surface forces such as van der Waals and electrostatic forces. In humid conditions, the formation of a meniscus also results in two additional forces, namely, surface tension and viscous forces. For contacting bodies under humid conditions and low surface roughness, these viscous forces are dominant [29,30]. Thus, it is possible that the surface forces alone can keep the balls within the interface if the size of the micro-bearing ball is below a critical value. For stationary condition, one can calculate the critical size of a ball below which the surface and viscous forces can hold the gravitational force. However, since the bearing, such as the one used in the present work, are supposed to spin at high rpm, we also calculate the centrifugal force that will be exerted on the ball and equate this force to the shear strength of the contact between the ball and the surface. Thus, theoretically it is possible to calculate the critical radius for a fixed rpm below which balls will not be dislodged out of the contact from a spinning disk. Although the above considerations can provide some design guidelines for selecting experimental parameters with respect to a given size of the ball, it should be noted that they do not take into account the load applied through the contacting surface as bearing ball rotates in between two surfaces. Our initial calculations have shown that the ball size of $53\,\mu m$ is well within the range of strong surfaces forces under high-humidity condition. In order to test the concept, for the present study we have used both with and without a wide channel for the micro-ball bearing. Our results show that it is important to have a wide channel on one of the Si plate to contain the micro-balls within this channel. For without channel bearing, the balls get out of the two Si plates because of the spiraling out due to very high number of rotations involved.

3. Experimental

3.1. Experimental set-up

The set-up (Fig. 1) consists of the rotary tribometer, a webcam attached to a microprocessor, and a humidity chamber for obtaining high-humidity condition. The motor, a brushless DC type, was obtained from Oriental Motor (Pte.) Ltd., Singapore. A gear head of gear ratio 1:25 was installed, giving the motor a rotational speed that ranged from 28 to 556 RPM. The start-up acceleration of the motor was kept constant. Dry borosilicate glass micro-spheres (GL-0179) of $53 \pm 3.7\,\mu m$ were obtained from MO-SCI Specialty Products, L.L.C., USA. Silicon (Si) wafers of $600\,\mu m$ thick were obtained from a local supplier, Engage Electronics Pvt. Ltd., Singapore. The surface roughness of the Si wafer was 0.41 nm, measured by AFM within a scan size of $10\,\mu m \times 10\,\mu m$. The average dead load acting on the top plate (TP) was fixed at $235\,\mu N$. The dead-weight load (item no. 2 in Fig. 1) may vary considerably if there is a tilt of the top plate (item no. 7). The bottom plate (BP) (item no. 8) was rotated using a brushless DC motor while the TP rested with glass micro-spheres in between. The spindle of the TP was fixed to a conventional deep groove ball bearing obtained from Koyo Seiko Co., Ltd. (Model: 6800ZZ JIS/ISO standards) which allowed for the freedom of rotation about the z-axis. Since the rolling friction of the surface micro-bearing is even lower than the macro bearing used for the TP, no torque can be measured under normal surface ball rolling conditions. Therefore during a normal run, the TP would remain stationary while the BP is being rotated by the DC motor with the micro-balls rolling in between. The rolling of the surface bearings results in extremely low friction between the Si substrates. However, TP rotation occurs intermittently when ball failure or Si plates rubbing at the edges causes momentary periods of high friction between the two Si disk plates and thus a torque high enough to rotate the TP is produced. As it is important for the rotating plate to have minimal wobble during the run, it is crucial to design for a wobble free rotating BP. This was achieved by using a simple method devised here to stick the BP onto a flat aluminum platform attached to the motor spindle. The surface of this platform, before sticking the BP, had been flattened by pressing down a sandpaper attached onto a flat surface using the z-axis while the motor was being rotated. This allowed for a flat platform for the silicon substrate. A double-sided tape was carefully attached to the platform. A pair of tweezers was used to carefully peel off the sticker before pressing the BP onto it. Now, to ensure that the TP will also have low relative wobble with respect to the BP, the TP must first be aligned with the BP. The TP was first adhered to the cap (item no. 5) using double-sided tape. The items were then pushed into the spindle cap (item no. 4) connected to the top bearing (item 3 in Fig. 1). The TP was then brought down to completely touch the BP. The TP now needs to be locked tight with the spindle. This was done by tightening two screws (item no. 6) around the cap. While doing so, alignment was ensured by constantly aligning the two plates together while the TP was rotated around for the screws to be tightened. When properly aligned, a strong adhesion force could be felt while trying to separate the contacting Si surfaces. To ensure proper alignment, this "force" was checked again at different TP orientations to finally ensure that they were in perfect parallel alignment.

3.2. Experimental procedure

New silicon plates (TP and BP) were attached for each new run. To remove any dirt on the silicon surface, an acetone soaked cotton wool was used to wipe the surface. The internal bearing (item no. 3 in Fig. 1(a)) of the TP was occasionally lubricated with oil to prevent it from failing inadvertently during the run. Care was taken to avoid the oil from dripping into the Si plates. To shape the silicon test plates into circular disks, $16\,mm \times 16\,mm$ Si wafers were adhered to the face of a cylindrical holder made of brass using double-sided tape, and the excess Si regions were

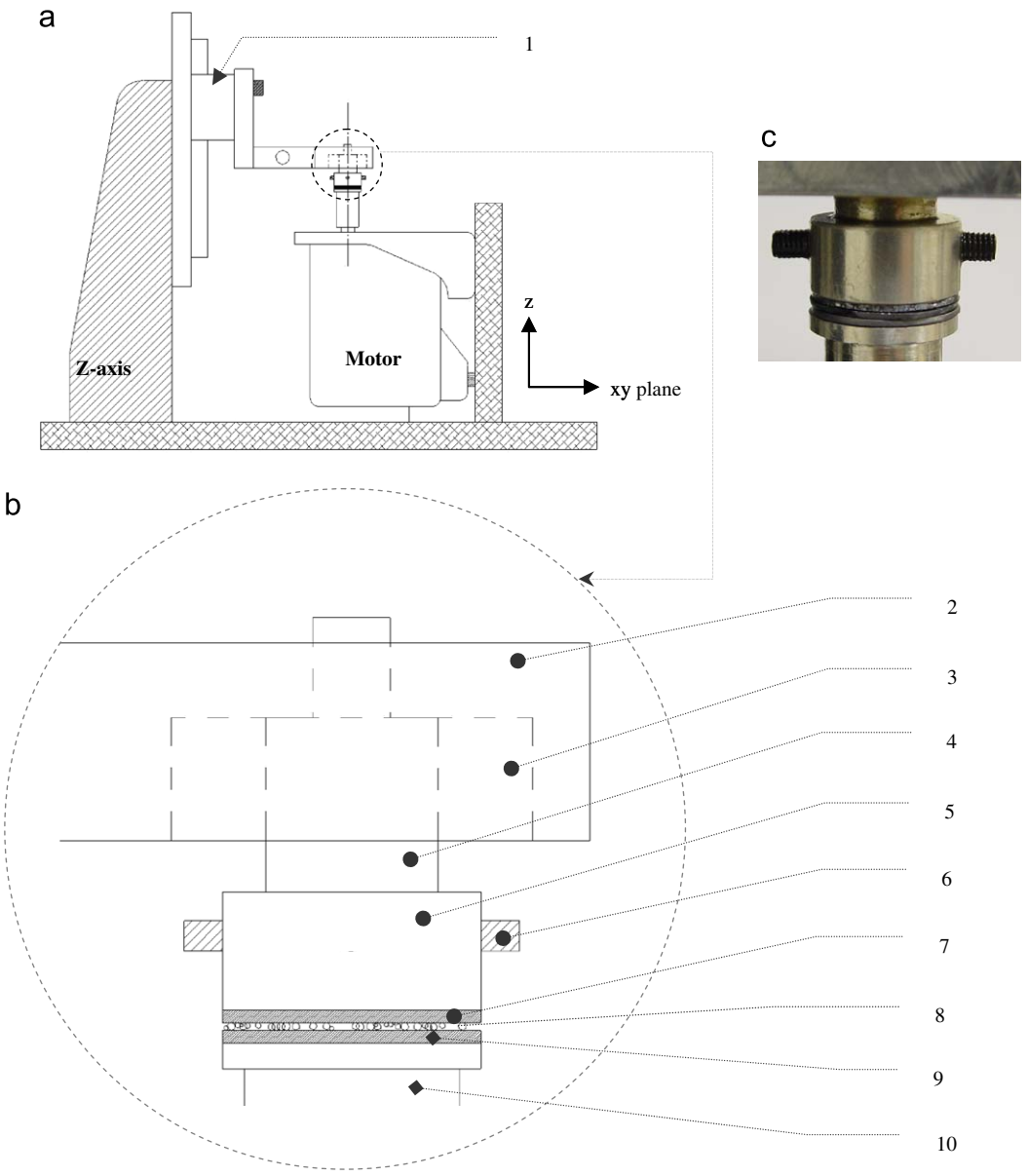

Fig. 1. (a) Schematic of the rotary tribometer. The humidity cover and webcam are not shown in the diagram. (b) Exploded view of the set-up near the top and bottom Si plates. *Legends*: (1) Movable stage connected to the *z*-axis. (2) Freely rotatable dead-weight load that rests on the surface bearings. (3) Deep groove macro-ball bearing, Model: 6800ZZ. (4) Spindle (free to rotate) attached to deep groove macro-ball bearings. (5) Cap on which TP is attached. (6) Screw to tighten cap (item no. 5) onto the spindle (item no. 4). (7) Top circular silicon plate (TP). (8) 53 ± 3.7 μm diameter glass micro-balls between the Si plates. (9) Bottom circular silicon plate (BP). (10) Aluminum cap permanently friction welded to motor spindle (drawings are not to scale). (c) Digital image showing the TP resting on the BP of the tribometer. The diameter of the Si plates is 15 mm.

ground away using a coarse grade sandpaper. Finer grade sandpaper could then be used to smoothen the edge of the disk. A protective layer of masking tape covered the Si disk during grinding to protect the surface from any scratches. Water was allowed to flow during the process to reduce heat generation and at the same time to remove the silicon debris. In order to create the circular channel (depth = 28 μm, width = 2.5 mm, and ID = 3 mm) on the bottom silicon plates, the following procedure was carried out. The test chips were fabricated in a cleanroom. The fabrication process was carried out on a P type (1 0 0) silicon wafer ($p = 10\,\Omega$ cm, thickness is 435 μm). The lithography process step defined both the silicon trenches and the scribing marks. After HMDS (hexamethyldisilazane) treatment, a 2 μm thick AZ 7220 (photoresist mask) was prepared on silicon wafer with the following process parameters (spin at 5000 rpm for 30 s, and bake at 95 °C hotplate for 30 s). An exposure was subsequently done by mask aligner (Karl Suss MA8 Mask aligner) with 12 s exposure at 10 mW/cm^2, and the exposed photoresist was then developed in AZ developer (1:1 to DIW) for 30 s. To keep the precise shapes of circular channel, no hard baking is performed after photoresist developing.

A deep silicon reactive-ion-etching (DRIE) was subsequently conducted with photoresist as the mask layer. The equipment used was Oxford Plasmalab ICP180 Etch system (Oxford Instruments). Both the circular channel and the scribing marks were precisely fabricated with the depth of 28 μm after DRIE process. The photoresist was subsequently removed by acetone and IPA. Chip Dicing was performed on DAD320 Dicing system (Disco). With the clear dicing marks, the silicon substrate was cut and the identical silicon chips were produced for further sample preparation.

To transfer the borosilicate ball bearings onto the flat silicon plate, a thin strip of paper was folded into half and used as an item to transfer, deposit, and disperse the balls. Weighing of the balls was first done by slowly depositing them carefully onto a silicon plate A (approximately 6 cm × 1.5 cm) that rested on an electronic weighing scale. In total, 22 (± 2) × 10^{-5} g of balls were used for all the runs. After weighing, the balls were transferred from plate A onto another Si plate B (approximately 6 cm × 1.5 cm). Dispersion was now done on plate B by lightly tapping the agglomerates with the strip, causing it to break up into smaller agglomerates and individual balls. Due to a high number of balls on a limited dispersion area on plate B, the efficiency of dispersion can be low. This will lead to poorly dispersed balls with high effective masses and a low dispersion factor (DF) (see Appendix 1 for the definitions of effective mass and DF). The poorly dispersed balls were transferred back to plate A again before finally depositing them onto the circular Si test plate. To achieve well-dispersed balls, the balls were first deposited onto only one half-portion of the plate B. The other unoccupied half-portion was used to disperse small portions of balls being brought over from the opposite side. The larger dispersion area now allows for a more effective dispersion. Chances of dispersed balls coming together again to recombine is also lesser. The small portion of well-dispersed balls was transferred to plate A for deposition onto the test plate. This was repeated until all the balls are deposited onto the test plate. The DF for poorly dispersed balls was 0.64, compared with 0.83 for the well-dispersed case. Fig. 2 shows samples of a well-dispersed (top left) and a poorly dispersed (top right) array of micro-balls on a Si plate.

To transfer the balls onto the silicon plates with channel, we dispersed balls onto the silicon surface, and used a piece of paper to sweep the balls into the channel. A micrograph image was taken to count the number of balls before deposition. The number of deposited balls ranged from about 100 to 200, with an average of 150 balls.

A humidity level of above 70% was used throughout the tests to achieve the capillary effect. After deposition of the balls, the dead-weight load (or TP) was brought down to gently rest on the balls. Next, an enclosure made using acrylic sheets, joined together by screws, was used to cover the tribometer from all sides. The humidity level in the chamber was raised by bubbling air into a bottle of water and feeding the bubbled air into the chamber. The RH was raised to about 85(± 1) % before the pump was switched off. The RH was then allowed to drop to a lower equilibrium level of about 75% before allowing the run to begin. This allowed relaxation of the glass microsphere's surface. A bottle of water was left in the chamber to keep the RH from dropping to below 70%. Due to this, the RH slowly crept up as the run progressed but stayed within 70–75%.

We conducted three sets of runs as shown in Table 1. Set 1 had a low DF (0.64). Set 2 had a high DF (0.84). The number of balls must be sufficiently large to keep the system stable during the run. Too few balls might result in the plates being unbalanced and tilted, causing the plates to rub and the run to fail. An average of 22 (± 2) × 10^{-5} g of glass balls were deposited each time. Some of the runs in Set 2 needed to be halted and continued next day due

Table 1
Experimental conditions for the 3 sets of life-cycle tests conducted.

Set	1	2	3
Dispersion factor (DF)	0.64 ± 0.05	0.84 ± 0.06	
	Low	High	High
Weight of balls (g)	22(± 2) × 10^{-5}		–
Number of balls	–		150(± 50)
Rotational speed (RPM)	300		500
Temperature (°C)	22(± 1)		

The RPM for Set 3 was increased slightly to achieve very large rotational cycles. This gave a linear speed in the channel of 78.5 mm/s. Rotational speed within this range did not affect the bearing life-cycle.

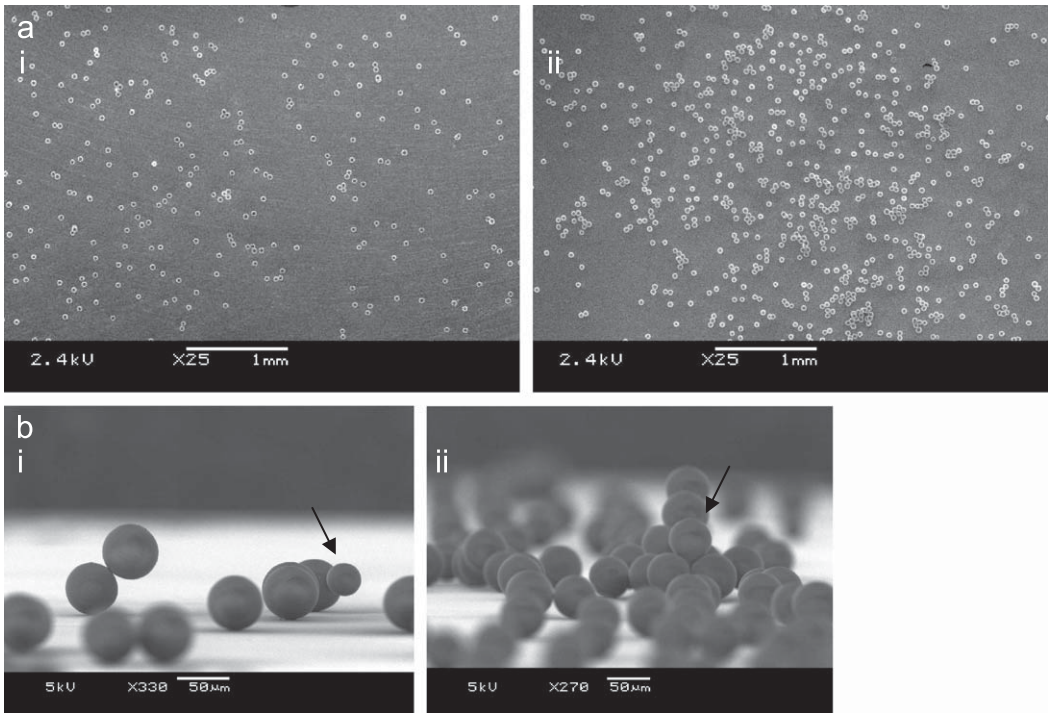

Fig. 2. (a)i Well-dispersed ball image taken by SEM showing majority of the spheres either singly or doubly agglomerated. (a)ii Poorly dispersed image showing majority of the spheres in large agglomerates. (b) SEM images showing balls adhered onto a Si substrate that is tilted almost vertical. (i) Image shows effective masses between 1 and 2, typical of a well-dispersed case. Indicated is also a ball that is deviant from the average diameter. (ii) Balls showing a variety of effective masses. The large agglomerates are typical of a poorly dispersed case.

to the long operating conditions. This start/stop did not seem to have any effect on the life-cycle. Set 3 studied the effect of a silicon plate with a circular channel 2.5 mm wide and 28 μm deep for the micro-balls to roll in. The purpose of the channel is to contain the balls in their rolling paths and to prevent them from rolling off the plates, as compared with the channel-less system.

To measure the long life-cycle, a digital webcam was used to record the whole run by using a time lapse function that captured an image at every 4 s interval. It was then converted into a video and could be analyzed later to determine the life-cycle. A run was considered to have failed when one of two things happened, namely, (i) when all the balls had completely left the surfaces. This occurred when the two plates came into contact which could be observed by the video image through the webcam, or (ii) when the TP persistently kept rotating due to rubbing of the silicon surfaces. This was an indication of high friction between the two plates that caused the TP to rotate along with the BP. As mentioned before, the TP has its own bearing (item no. 3 in Fig. 1) fixed to its spindle that is free to rotate upon small torque.

The coefficient of friction in rolling for the micro-balls was measured on a traditional tribometer (Center for Tribology, CETR, USA) in linear translation. Approximately 20–30 glass micro-balls were deposited with very high dispersion onto a silicon plate (10 mm × 20 mm) (bottom plate) that was fixed to the tribometer using double-sided adhesive tape. The top Si plate was approximately 10 mm × 10 mm in dimension which was carefully brought on top of the glass ball deposited bottom plate. This free placement of the top plate ensured perfect alignment of the two plates with micro-balls in between them. Both Si plates were cleaned with acetone prior to use. The force sensing arm of the tribometer with a spherical tip was gently brought down to touch the top surface of the top plate and finally a very light load (a few grams) was applied through this sensor onto the top plate. The spherical tip of the force sensing arm was then fixed with the top plate while in contact by releasing a few drops of super glue to the region of the contact with the top plate. The glue was allowed to set for approximately 15 min. Thus, the top plate was now fixed to the force sensing arm of the tribometer. The above process ensured that the bottom and the top plates were in excellent alignment before friction test. The bottom plate was moved in translation motion during the friction test and the top plate remained stationary giving normal and friction force data.

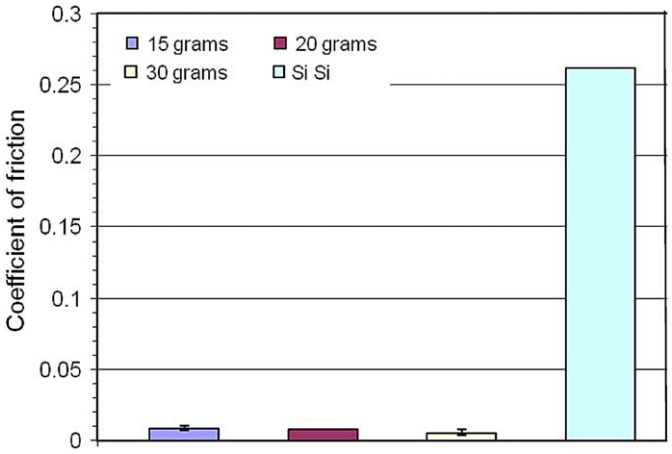

Fig. 3. Coefficient of friction in rolling test for glass balls between two silicon plates. The tests were conducted at different normal loads applied. The rolling coefficient of friction was in the range of 0.005–0.008 with very little data scatter as shown in the plot. The bar for Si–Si indicates the (pure sliding contact) coefficient of friction between Si plates without any glass ball in between when the normal load was 15 g.

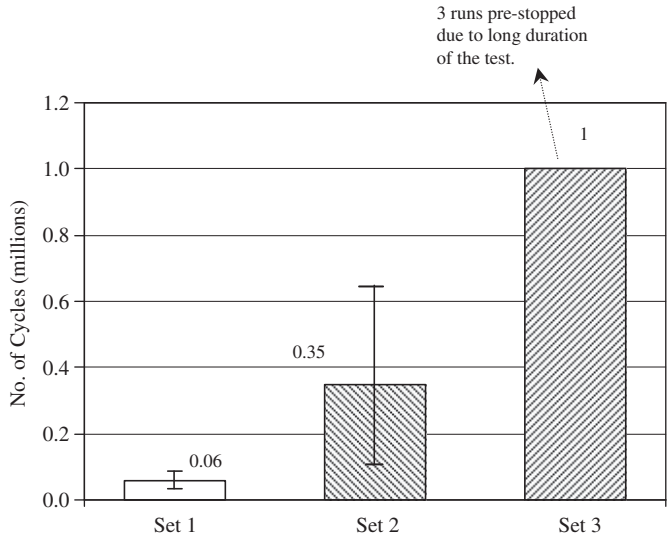

Fig. 4. Life-cycles of run for the three cases. Sets 1 and 2 have an average life-cycle of 0.06 and 0.35 millions, respectively. Set 3 has a life-cycle consistently above 1 million cycles for three test repeats.

4. Results and discussion

4.1. Rolling friction data

Fig. 3 gives the data for the coefficient of friction for micro-balls in rolling contact. Normal load was varied within a limited range to observe any normal load effect. Si-on-Si was also slid, without the micro-balls in between (pure sliding), for comparison purpose. The coefficient of friction for Si-on-Si without micro-balls is extremely high (0.26) which confirms that Si is a very poor tribological material. The average coefficients of friction for the micro-ball bearing tests were 0.008, 0.007, and 0.005 for 15, 20, and 30 g normal loads, respectively. These data are average values of several repeats of the tests with the bottom plate moving back and forth in linear fashion. The coefficient of friction for micro-balls is extremely low (by an order when compared with the literature value for similar micro-bearings) and suitable for bearing application. There is slight effect of the normal load. The coefficient of friction for higher load is slightly low. One reason for this slight drop in the coefficient of friction is the change in the slide-to-roll ratio, however, this is not possible to confirm in the current set-up. Another reason may be because glass material responds to pressure and shows some liquidus material at the contact when pressure is applied (this is explained later). The coefficient of friction, nevertheless, is very low for all loads used which proves that the rolling mechanism in micro-ball bearing is effective.

4.2. Life-cycle data

The life-cycles of the three sets are summarized in Fig. 4. Several runs for each set are averaged to give a mean value for each set. Sets 1 and 2 that compare the difference in the dispersion factor have an average life-cycle of 0.06 and 0.35 millions, respectively. Set 3, for the channeled bottom plate, has life-cycles consistently above 1 million cycles for every test repeat. As can be seen from the data, there is wide data scatter even for the high DF runs (Set 2) when there is no channel on the bottom plate.

4.2.1. Set 1: poorly dispersed balls (low DF), flat silicon plates

Observation of the Si surface under optical microscope for Set 1 after the balls had completely left the surface (complete failure) shows evidence of brittle-like failure as well as adhesion failure. Glass debris and ball tracks are formed as seen in Fig. 5. Fig. 5(a) shows some glass-like debris, believed to be due to rolling cyclical fatigue and fretting. The glass-like stains shown in Fig. 5(b) are adhesion marks on the wear track, believed to have been caused by softening of the micro-ball surface after prolonged rolling cycles. Under the inverter image, the glass debris appears as bright spots whereas the adhesion stains do not appear as bright under the same magnification, as seen in Fig. 5(bi). The difference could be because the glass has undergone plastic flow together with some physical and chemical changes for the stains, which alters the optical and physical characteristics, and hence, does not reflect the light as well when compared with the debris which are broken pieces of the glass balls. Thus, for Set 1, failure takes place by the breakages of the balls (as evidenced by glass fragments) and melting due to softening of the glass material (as evidenced by plastically deformed stains on the Si surface).

4.2.2. Sets 2: well-dispersed balls, flat silicon plates (high DF)

Set 2 is the set where the balls are well-dispersed (high DF). The DF is the critical factor differentiating this run from Set 1, and is evident by the longer average life-cycle.

The large scatter in Set 2 may be due to the uniqueness of the distribution of each run; it is extremely difficult to obtain same DF in each run. Furthermore, the way the balls dynamically organize themselves while rolling in each run can be unique. It is also possible that for Set 2, and also Set 1, some glass balls fell off the bearing surfaces leading to lesser number of balls to support the plates and thus accelerated wear. The falling of the balls was confirmed by placing a paper below the set-up where fallen balls were collected. This is because of the spiraling out of the balls due to very large number of rotational cycle. Lesser number of balls may increase the chance of the contact between the top and bottom plates at outer edges.

4.2.3. Set 3: balls rolling within channeled silicon plate (bottom) (high DF)

For Set 3, a circular channeled (channel dimensions: depth = 28 μm, width = 2.5 μm and ID = 3 mm) bottom silicon plate and a flat top silicon plate are used. As the region for the balls to roll is limited to the channel, lesser balls are used. The life-cycles of all the runs exceeded 1 million cycles and the tests were stopped without failure due to long test duration. From the results for this set, it is immediately clear that the channel acts as a barrier to prevent the balls from rolling out. We did not find balls falling outside the circular Si plate. Thus, the life of the bearing is satisfactorily increased, as the balls do not get removed from the interface during dynamic interaction. Occasional glass melts (see the next section) are also observed in the channel that is within the ball rolling path, which does not seem to affect the friction coefficient of the system or the bearing life.

4.3. Further analysis

Due to the longer rolling cycles of Sets 2 and 3, melting at the surface of the ball can occur (Fig. 6). It has been reported in the literature [31,32] that under conditions of high humidity and contact pressure, the surface of glass undergoes changes that lowers its viscosity, known as "hydrolytic weakening effect". This lowering of glass viscosity effect is similar to the effect of melting as it makes the glassy phase more mobile. As both these conditions are prevalent in all the runs, it accounts for the observed phenomenon. High temperature is not the only factor for the lowering of the glass viscosity. Fig. 7(a) shows some viscous-looking glass stains when the glass micro-spheres are in between a glass and a silicon piece and some pressure is applied with gentle rolling of the balls. The melt layer of the glass that forms on the silicon surface due to pressure can act as a mixed lubricating layer separating the ball and the substrate. Hence, this could contribute to higher life-cycle. Fig. 7(b)–(d) shows FE-SEM images of the solidified glass melts on the Si surface in Set 3. Fig. 8 shows the EDX profile of the solidified glass-melt images. The glass ball debris is confirmed by the presence of Al and O in addition to Si. These glass debris is believed to increase wear due to abrasive action when in solid form, however, in semi-solid or liquid form, they can have lubricating effect. This could be the reason for extremely high rolling cycles despite the fact that molten glass stains were found inside the channel area.

To explain why the life-cycle for Set 1 is the lowest, we introduce and define the concept of dispersion factor. Set 1 has a lower DF than Set 2. A lower DF implies that there are many clusters of balls with a high effective mass (see Fig. 2(b)i and ii). Due to the strong surface forces acting, colliding balls adhere together upon contact. Therefore, a node contacting into a rolling ball can cause the ball to stick to it, increasing its effective mass. The nodes account for the rapid dislodge of the balls from the silicon plates as well. In conclusion, a high dispersion factor leads to lower effective masses and consequently, a longer life-cycle.

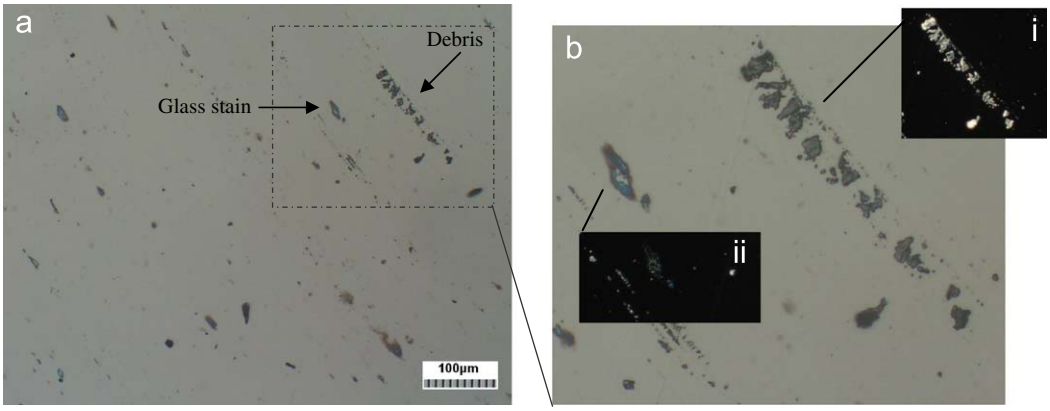

Fig. 5. (a) Micrograph image of glass debris and glass stains. (b) A further magnified image (3 ×) of the debris and stain. (bi) Inverted image of glass debris showing up as bright spots. (bii) Inverted image of stains do not show up as bright.

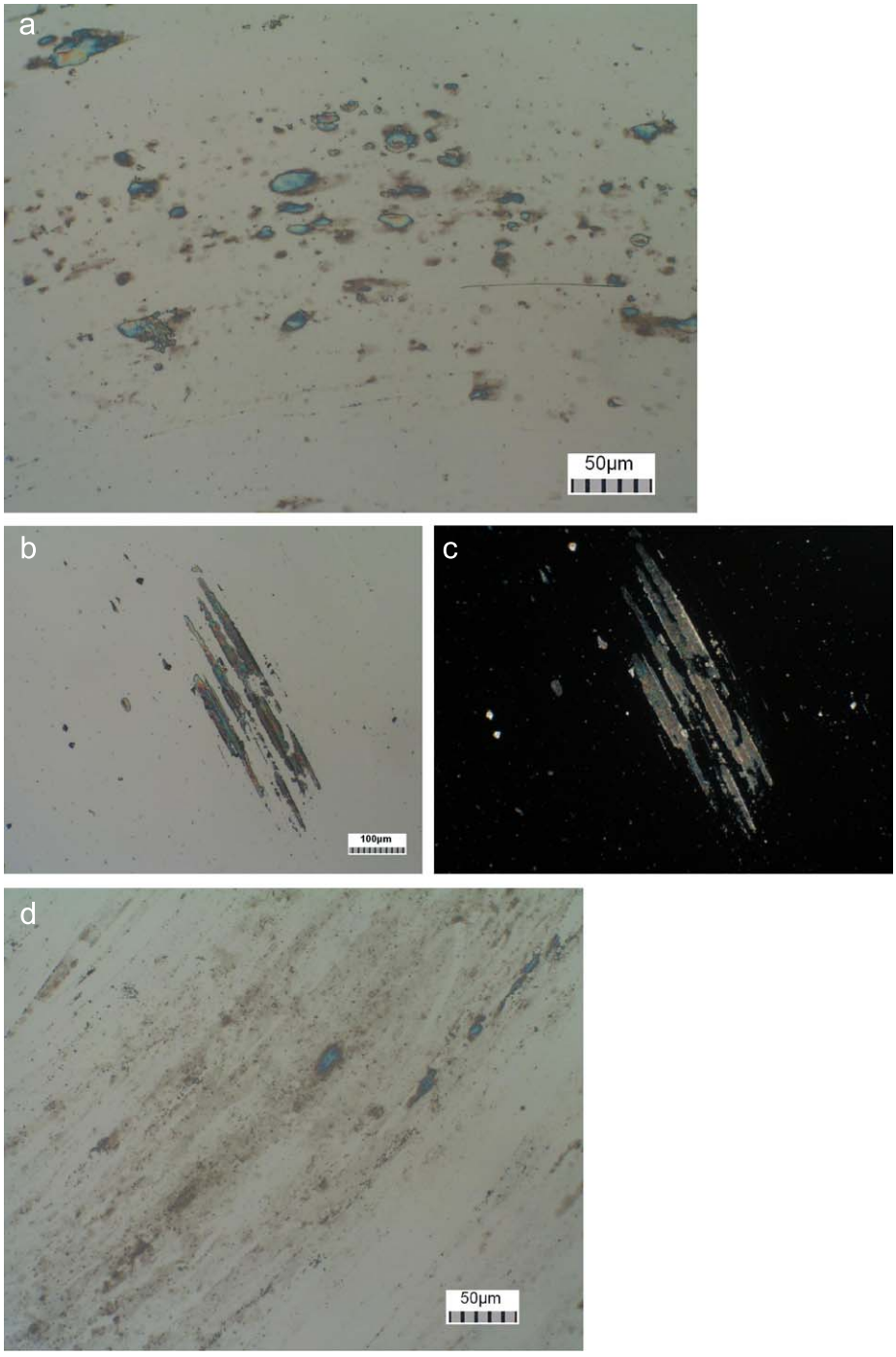

Fig. 6. (a) Glass-melt stain believed to have lubricating effect. The images are taken near the center of the disk. (b) A severe looking stain that is taken further away from the center that could have been formed probably due to the high load and speed at the instant. (c) Inverted image of (b) showing difference in the melt stain and broken glass ball debris on the surface. (d) Micrograph shows glass stains forming a "carpet" layer on the Si surface.

4.4. Factors affecting the life-cycle

From the present study, we can conclude that there are some important factors that need to be controlled in order to make micro-ball-bearing technology a viable option. These factors are briefly discussed below.

4.4.1. Alignment and stability of test plates

The alignment of the two (Si) plates or surfaces is a prerequisite for any of our life-cycle tests to be meaningful. A large wobble of either the BP or TP will result in Si plates rubbing at the edges, causing high friction and rapid ball dislodge. This type of instability of test set-up has been reported by Beerschwinger et al. [15] in earlier linear tests, hence, resulting in a poor life-cycle.

Another challenge to alignment is the variance in the size of the balls. Due to a size variance, the TP resting on the balls might be tilted at an angle. A probability exists for the TP to actually come into contact with the BP near the edges. If this happens, rubbing will occur during the run resulting in high friction and a quick dislodge of the balls. Occasionally, this also leads to a

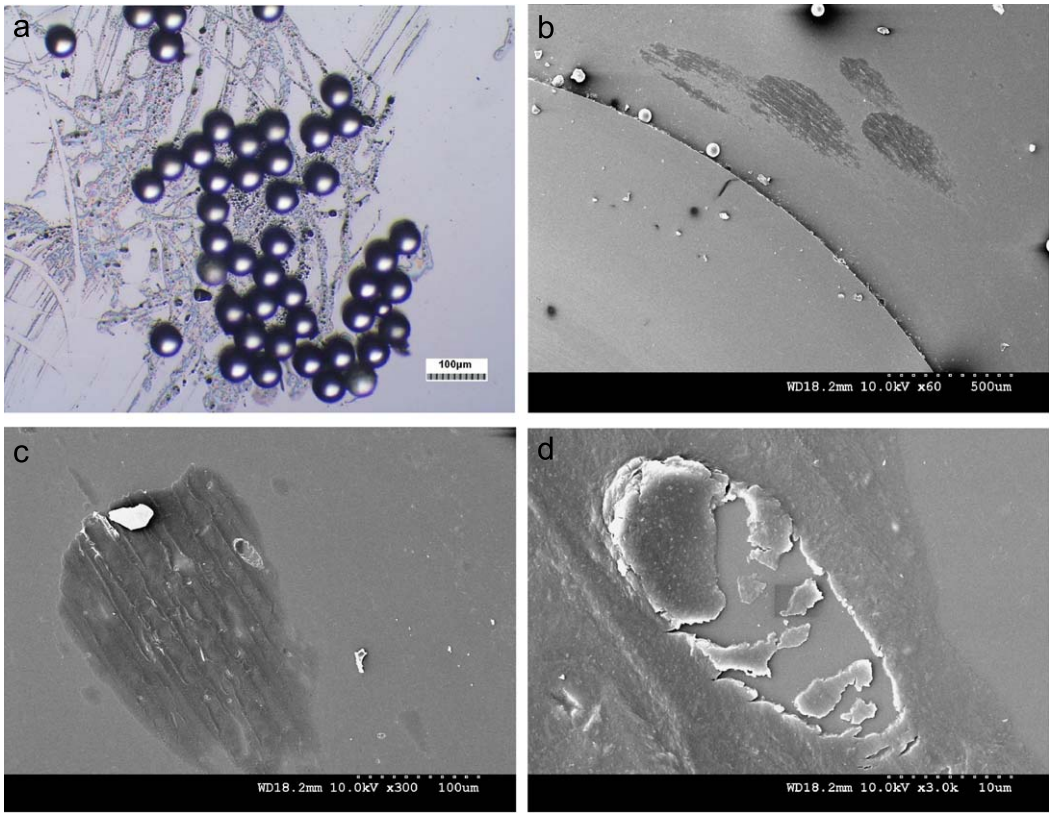

Fig. 7. (a) Micrograph image showing low viscous-glass-melt stains on silicon surface when pressure is applied to the glass balls and rolled gently. The melt layer separates the ball from the silicon surface, and is believed to have some lubricating effect. (b) FE-SEM imagines of glass-melt stains. (c) Glass-melt stain and solid glass debris. (d) High-magnification image at a spot on the glass stain, showing the fracture/shearing of the softened glass.

wobbling motion of the TP. Using ball bearings of a more uniform size distribution will reduce this problem. Such factors need to be seriously considered when conducting life-cycle tests and when implementing the micro- or nano-sized surface bearings in the future. The problem of alignment will become even more severe as the ball diameter is further reduced. Prior application of a solid lubricant to the Si plate surface may help in this regard [33]. This will eliminate the use of any liquid lubricant as micro-systems are not very suitable for liquid lubrication due to large viscous drag and stiction problems.

4.4.2. Channel

The channel for the bearing balls acts as barrier to prevent the balls from rolling off the plates. The balls rolling in the channel in Set 3 clearly shows that it greatly helps prevent balls from rolling off the plates. This type of channel is easier to fabricate by wet-etching method and even few micron diameter ball can be deposited in a channel without much problem. The only role of the channel is to contain all the balls within its two walls during the rolling operation. Our study has clearly shown that micro-ball-bearing technology without channel has lesser life-cycle. Unlike individual groove for balls, wide channel does not require any extra step of confining the balls to a groove as all balls are free to move within one wide channel.

4.4.3. Dispersion factor

For runs conducted on flat silicon surfaces, DF after deposition greatly affects the life-cycle and there is a positive relationship between DF and life-cycles. During the run, balls can still agglomerate together, and effective mass can increase. Hence, ways to prevent or reduce the agglomeration of the balls will be useful. Some chemical surface modification of the ball to make them slightly hydrophobic may have beneficial effect in avoiding unnecessary agglomeration of the micro-balls due to strong surface forces.

5. Conclusion

Micro-ball bearing has been tested with balls rotating between two 15 mm diameter Si plates, with and without a channel on one of the plates. In total, $53 \pm 3.7\,\mu m$ glass micro-spheres rolling between two silicon plates in relative motion reduce the coefficient of friction to as low as 0.005 and increase bearing life. The surface bearings exhibit extremely low coefficient of friction due to rolling action. The rolling life-cycles exceeding 1 million is consistently obtained when the balls are rotated between two Si plates with one of the plates having a wide channel. Such a channel helps to keep all the balls within the boundaries giving low coefficient of friction throughout the run. Important factors such as critical ball radius (R_c), presence of a channel, dispersion factor, two plate surface alignment, and the critical number of balls and their distributions, are all crucial in affecting the life-cycle of the micro-ball bearing. Lastly, the low cost of the micro-spheres coupled with their attractive tribological properties make them suitable candidates for the reducing wear in micro-mechanical devices.

Acknowledgements

This work was supported by the NUS Nanoscience and Nanotechnology Initiative (NUSNNI) research Grant #R-265-000-132-112.

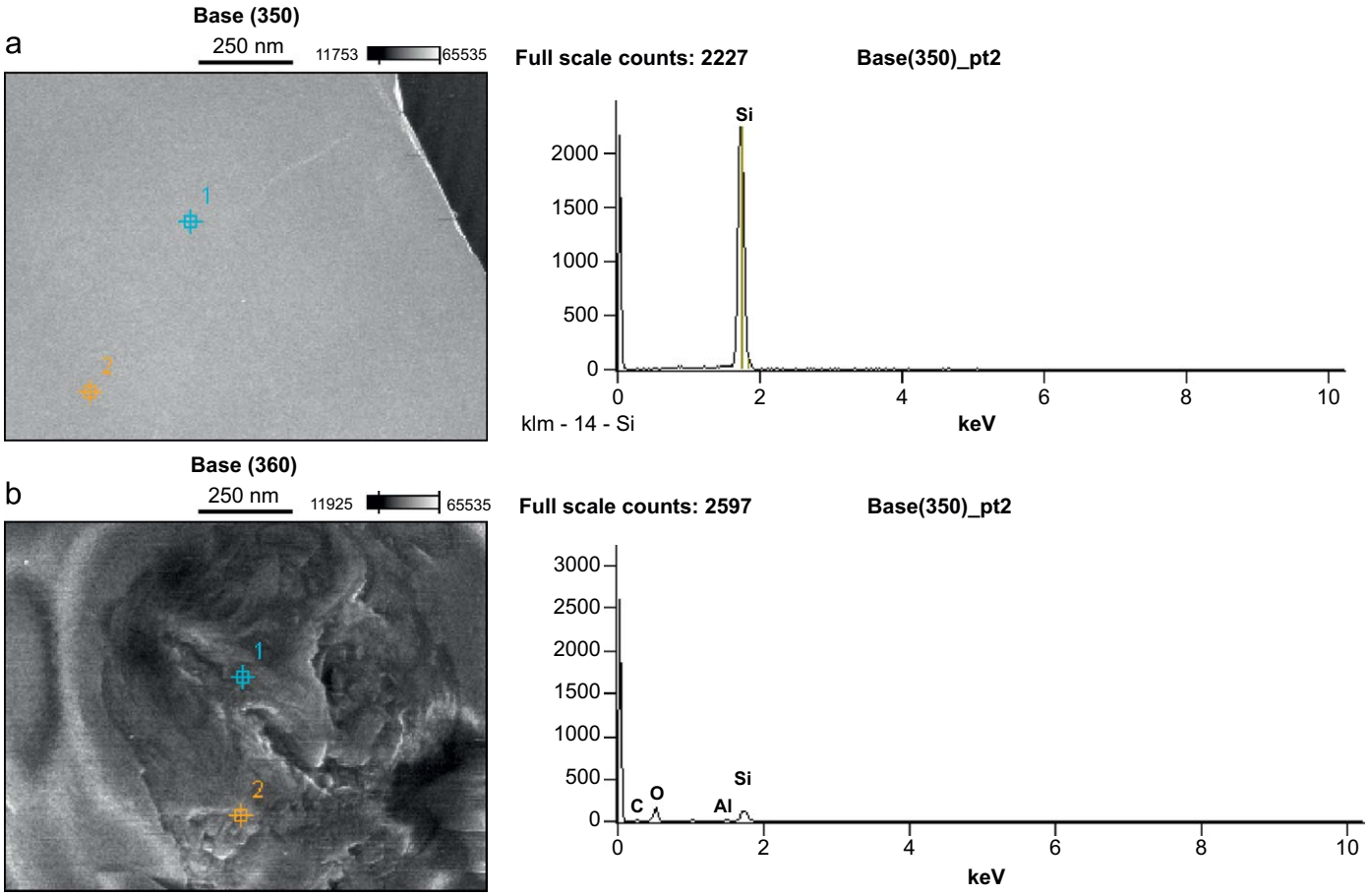

Fig. 8. EDX of (a) bare silicon surface. (b) Glass micro-sphere debris on inside the channel. The presence of Al and O are indicative of the glass.

Disclaimer

Names of companies and suppliers have been included in the paper for information only and this does not represent endorsement of their products. Views expressed in this paper are those of the authors only.

Appendix 1

Dispersion factor and mean the effective mass ($\bar{x}$) are quantities that can be used to describe the quality of the dispersion of deposited bearing balls on the bottom plate. Due to the large surface to volume ratio of the balls, the strong surface force causes agglomeration of the balls. To quantify this effect, we introduce the above two quantities.

The relationship between DF and $\bar{x}$ is given as by

$$DF = (\bar{x})^{-1}$$

$\bar{x}$ is determined by counting and averaging the mean size of the balls and agglomerates deposited on the Si plate. To get DF values for poorly dispersed and well-dispersed cases, we emulate actual deposition conditions by weighing $22(\pm 2)\times 10^{-5}$ g of balls and depositing them on the Si substrate used for a BP using the methods described in the paper. Five to seven SEM images are then taken using magnification of about $27\times$. To tabulate the frequency of the various mean masses, we print out the image and strike out the balls/agglomerates as effective masses and its frequencies of occurrences is noted. The data for the images taken to represent the dispersion of the particular plate is tabulated using an Excel spreadsheet, and the mean effective masses for the images is calculated by the formula, given as

$$\bar{x} = \frac{\sum_1^N x_i f_i}{\sum_1^N f_i} \quad \text{where } 1 \le i \le N$$

Here, x represents the number of balls in a particular agglomerate where the subscript i denotes the number ($i = 1$ means the ball is singly dispersed, and $x_7 = 7$), f is the frequency of occurrence (e.g., f_7 is the number of times counted for the agglomerate of size of 7 balls), and N represents the largest observed agglomerate size. For poorly dispersed balls, N is around 12–15 while it is around 5 for well-dispersed balls.

To avoiding double counting, overlap regions of the images are struck out. A ballpoint pen is used to mark the locations on the Si plate. Deliberately imaging with the pen mark can help to identify regions of overlap. Three samples for each dispersion mode are taken. The respective effective masses for the plates are averaged to provide an estimate for the DF. The DF for poorly dispersed is 0.64 ± 0.05, and is higher for well-dispersed, at 0.83. As we approached DF of 1, we start getting more singly dispersed balls. A DF of 1 means that there is no agglomeration and that all the balls are dispersed perfectly.

References

[1] Maboudian R, Robert Ashurst W, Carlo Carraro. Tribological challenges in micromechanical systems. Tribology Letters 2002;12(2).
[2] Tanner DM, et al. MEMS reliability, infrastructure, test structures, experiments, and failure modes. SAND2000-0091, Unlimited release, January 2000.
[3] Walraven JA. Failure mechanisms in MEMS. In: ITC international test conference, Paper 33.1, p. 828.

[4] Williams JA, Le HR. Tribology MEMS. Journal of Physics D: Applied Physics 2006;39:R201–14. See here: http://www.iop.org/EJ/abstract/0022-3727/39/12/.
[5] de Boer MP, Mayer TM. Tribology of MEMS, MRS bulletin, April 2001.
[6] Bhushan B, Liu H, Hsu SM. Adhesion and friction studies of silicon and hydrophobic and low friction films and investigation of scale effects. Journal of Tribology 2004;126:583.
[7] Gellman AJ. Vapor lubricant transport in MEMS devices. Tribology Letters 2004;17(3).
[8] Williams JA. Friction and wear of rotating pivots in MEMS and other small scale devices. Wear 2001;251:965–72.
[9] Tanner DM, Walraven JA, Irwin LW, Dugger MT, Smith NF, Eaton WP, et al. In: IEEE international reliability physics symposium, March 21–25, San Diego, CA, 1999. p. 189–97.
[10] Maboudian R. Surface processes in MEMS technology. Surface Science Reports 1998;30:207–69.
[11] An Introduction to MEMS, Prime Faraday Technology Watch, January 2002.
[12] Babcock W, Rose D. Materials challenges for the MEMS revolution. The AMPTIAC Newsletter, vol. 5(1).
[13] Zabinski JS. Failure mechanisms of a MEMS actuator in very high vacuum. Tribology International 2002;35:373–9.
[14] Kim D, Cao D, Bryant MD, Meng W, Ling FF. Tribological study of microbearings for MEMS applications. Journal of Tribology 2005;127/537.
[15] Beerschwinger U, Reuben RL, Yang SJ. Frictional study of micromotor bearings. Sensors and Actuators A—Physical 1997;63:229–41.
[16] Kang JW, Hwang HJ. Fullerene nano ball bearings: an atomistic study. Nanotechnology 2004;15:614–21.
[17] Chiñas-Castillo F, Spikes HA. Mechanism of action of colloidal solid dispersions. Journal of Tribology 2003;125:552.
[18] Rapoport L, et al. Hollow nanoparticles of WS2 as potential solid-state lubricants. Nature 1997;387:791.
[19] Rapoport L, Volovik Y, Leshchinsky VM, Nepomnyashchy O, Tenne R. Mechanism of friction of fullerenes. Industrial Lubrication and Tribology 2002;54(4):171–6.
[20] Braun OM. Simple model of microscopic rolling friction. Physical Review Letters 2005;PRL95:126104.
[21] Geiger M, Goode H, Ohanlon S, Pieloch S, Sorrells C. Glass microsphere lubrication. NAS 1.26, 197157, 1991. p. 85.
[22] Ghodssi R, Denton DD, Seireg AA, Howland B. Rolling friction in a linear microstructure. Journal of Vacuum Science and Technology A 1993;11:803–7.
[23] Lin TW, Modafe A, Shapiro B, Ghodssi R. Characterization of dynamic friction in MEMS-based microball bearings. IEEE Transactions on Instrumentation and Measurement 2004;53(3).
[24] Tan X, Modafe A, Hergert R, Ghalichechian N, Shapiro B, Baras JS, et al. Vision-based microtribological characterization of linear microball bearings. In: Proceedings of the 2004 ASME/STLE international joint tribology conference, Long Beach, CA, USA, October 24–27, 2004.
[25] Miura K, Kamiya S. C60 molecular bearings. Physical Review Letters 2006;90(5).
[26] Mantiziba F, Gory I, Skidmore G, Gnade B. Wet-etch release process for silicon-micromachined. Journal of Microelectromechanical Systems 2005; 14(3).
[27] Wiles JA, Whitesides GM. Dynamic self-assembly of rings of charged metallic spheres. Physical Review Letters 90(8).
[28] Falvo MR, Taylor RM, Helser A, Chi V, Brooks Jr. FP, Washburn S, et al. Nanometre-scale rolling and sliding of carbon nanotubes. Nature 1999;397.
[29] Rabinovich YI, Adler JJ, Madhavan SE, Ata A, Singh RK, Moudgil BM. Capillary forces between surfaces with nanoscale roughness. Advances in Colloid and Interface Science 2002;96:213–30.
[30] Fisher LR, Israelachvili JN. Direct measurement of the effects of meniscus forces on adhesion: a study of the applicability of macroscopic thermodynamics to microscopic liquid interfaces. Colloids and Surfaces 1981;3(4): 303–19.
[31] Shang H, Rouxel T, Buckley M, Bernard C. Viscoelastic behavior of a soda-lime-silica glass in the 293–833 K range by micro-indentation. Journal of Materials Research 2006;21(3):632–8.
[32] Shang H, Rouxel T. Creep behavior of soda-lime glass in the 100–500 K temperature range by indentation creep test. Journal of the American Ceramic Society 2005;88(9):2625–8.
[33] Satyanarayana N, Sinha SK, Ong BH. Tribology of a novel UHMWPE/PFPE dual-film on Si surface. Sensors and Actuators A—Physical 2006;128(1):98–108.